
# Volatile resistive switching in Cu/TaOx/-Cu/Pt devices

Tong Liu, Mohini Verma, Yuhong Kang, and Marius Orlowski

Citation: Applied Physics Letters **101**, 073510 (2012); doi: 10.1063/1.4746276
View online: http://dx.doi.org/10.1063/1.4746276
View Table of Contents: http://scitation.aip.org/content/aip/journal/apl/101/7?ver=pdfcov
Published by the AIP Publishing

# Volatile resistive switching in Cu/$TaO_x$/$\delta$-Cu/Pt devices

Tong Liu, Mohini Verma, Yuhong Kang, and Marius Orlowski
*Bradley Department of Electrical and Computer Engineering, Virginia Polytechnic Institute and State University, Blacksburg, Virginia 24061, USA*

(Received 21 February 2012; accepted 1 August 2012; published online 17 August 2012)

A volatile switching of conductive filament (CF) in a Cu/$TaO_x$/$\delta$-Cu/Pt device has been observed. The device differs from a conventional Cu/$TaO_x$/Pt device by the insertion of a thin Cu-layer ($\delta$-Cu) between the electrolyte and the inert electrode. The Cu CF is formed the same way as in the conventional nonvolatile devices. However, when applied voltage becomes zero, CF ruptures spontaneously. The dynamic balance between $Cu^+$ field-supported hopping transport and the Cu self-diffusion explains the effect of CF volatility. The device can operate reliably in volatile and nonvolatile modes. © *2012 American Institute of Physics*. [http://dx.doi.org/10.1063/1.4746276]

Resistive switches suggested in the past as a replacement of non-volatile random access memory[1] and as the switching elements in reconfigurable logic circuits,[2] are making now inroads in stateful logic operations,[3] neural networks,[4] and chaotic circuits.[5] The resistive switching devices are based on the existence of a low resistance state (LRS) and a high resistance state (HRS).[1] Crucially, both states are stable and non-volatile. In this paper, evidence of volatile resistive switching is presented. Volatility of the conductive filament means that once the conductive bridge has been formed at a finite voltage $V_{set}$, the device remains in LRS as long as the same polarity voltage is maintained. As soon as the applied voltage is zero or close to zero, the device reverts spontaneously to the HRS. Hence, the low resistance state, characterized by existence of the conductive filament, is only dynamically stable as long as high enough voltage is applied to the device.

The schematic of device cross-section is shown in Fig. 1(a). The difference to the conventional resistive switch is the insertion of a thin Cu layer ($\delta$-layer) interposed between the solid electrolyte and the inert Pt electrode. We have fabricated Cu/$TaO_x$/$\delta$-Cu/Pt switches at room temperature with 32 nm thick oxygen-deficient $TaO_x$ formed by e-beam evaporation. The bottom Pt electrode has been deposited by evaporation and patterned by lift-off on a thermally oxidized Si wafer. The top Cu electrode lines were processed in the same way but patterned perpendicularly to the bottom Pt lines. The width of the metal lines varies between 1 $\mu$m and 35 $\mu$m. With the exception of the Cu $\delta$-layer, the manufacturing process is the same as in Ref. 6. The thickness of the Cu $\delta$-layer between $TaO_x$ and Pt bulk electrode is 6.5 nm.

Since the sample has been processed at room temperature it is believed that $\delta$-Cu layer should stay intact after processing of the full layer stack because of low Cu diffusivity in $TaO_x$ at 300 K. This is also supported by data of Liu[7] showing that an RTP step at 600 °C is needed to diffuse Cu in a 40 nm $ZrO_2$ layer. Fig. 1(b) shows 15 consecutive volatile switching cycles of a Cu/$TaO_x$/$\delta$-Cu/Pt cell. As soon as the voltage is swept to zero, the nanofilament dissolves spontaneously, rendering a RESET operation for the transition from LRS to HRS unnecessary. The measured HRS to LRS ratio is $10^2$ to $10^5$.

We postulate that the reason for the spontaneous dissolution of the conductive filament (CF) is an upset balance between the field-supported $Cu^+$ flux ($F_{Cu}{}^+$) and the self diffusion flux of Cu ($F_{Cu}$) in the CF and through the interface between the Cu bridge and the Cu $\delta$-layer on the Pt electrode as shown conceptually in Fig. 2(a). In the absence of Cu $\delta$-layer (i.e., the case of conventional devices), the Cu diffusion flux at the interface of CF with Pt electrode is null because of the inert electrode's ion stopping power. When the device is in the set condition, where the cell transitions from HRS to LRS state, only the flux $F_{Cu}{}^+$ is significant. The $F_{Cu}$ flux, which may deplete Cu atoms from the bridge, exists only at the tip of the bridge touching the Cu electrode. Since the radius of the contact cross-section between the filament and Cu electrode is less than 10 nm, $F_{Cu}$ must be perforce small. Hence, while operated in the positive voltage regime the bridge tends to strengthen decreasing its resistance in the process. The insertion of Cu $\delta$-layer enables a Cu diffusion flux from the established Cu bridge at its broad base (opposite end to the tip of the bridge) into the $\delta$-layer and the flux is additionaly enhanced by the elevated local temperature resulting from Joule heating. Thus the bridge at the interface with Cu $\delta$-layer is enhanced both by geometry of the bridge and by the thermal effect. This Cu self-diffusion flux ($F_{Cu}$) tends to remove Cu from the CF. If the removal of Cu is larger than the incoming $Cu^+$ flux ($F_{Cu}{}^+$), the CF is bound to dissolve. For 5 nm to 8 nm Cu $\delta$-layers, a thicker Cu $\delta$-layer may lead to larger $F_{Cu}$. The dependence on $\delta$-layer thickness will be noticeable only for 5 nm to 8 nm Cu $\delta$-layers. Beyond a critical thickness, the $F_{Cu}$ flux will cease to depend on the thickness of the $\delta$-layer and would start to behave like a bulk Cu electrode.

To verify this hypothesis, we have manufactured Cu/$TaO_x$/Cu devices and confirmed that Cu bridge formation cannot be observed. The Cu atoms of CF formation dissolve quickly in the Cu counterelectrode. To test this hypothesis of Cu self-diffusion flux further, voltage for the SET operation for the $\delta$-Cu devices has been swept in positive direction and then back toward zero. However, before reaching 0 V, the voltage sweep has been suspended at a finite voltage and let sit for some time. The results of the interrupted sweep are shown in Fig. 2(b). For curves 1 and 2, the negative sweep has been halted at 0.2 V and 0.15 V, respectively. An abrupt current drop can be observed

 

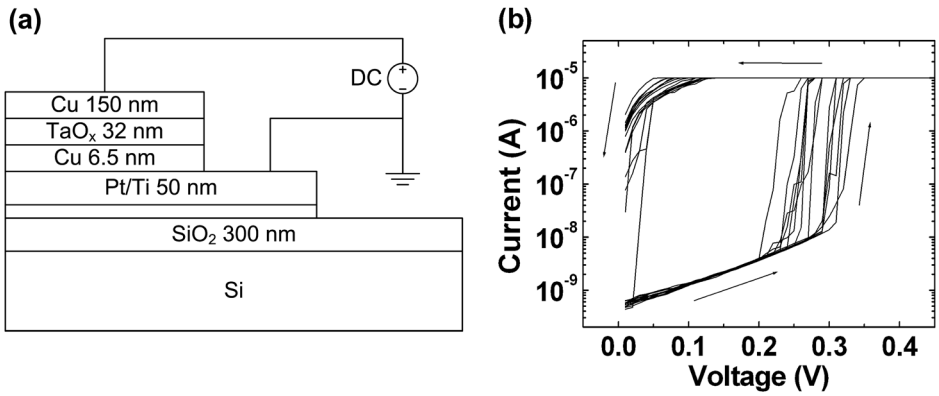


FIG. 1. (a) Cross-sectional view of Cu/$TaO_x$/$\delta$-Cu/Pt volatile resistive switching cells. (b) Fifteen consecutive volatile switching curves of a Cu/$TaO_x$/$\delta$-Cu/Pt device in log scale.

(equivalent to Cu bridge resistance increase) but stabilizes at a lower value indicating an unruptured Cu bridge with higher $R_{on}$ resistance. CF appears to stabilize itself by increasing $R_{on}$, thus reducing the current, Joule heating, and, by extension, $F_{Cu}$. For curve 3, however, the negative voltage sweep has been halted at 0.1 V, and the resistance increased to the $R_{off}$ state, indicating that CF has ruptured. In case of curves 1 and 2, the voltage across the electrolyte is still large enough to support $F_{Cu}{}^{+}$ that is larger than the $F_{Cu}$. However, for curve 3, $F_{Cu}{}^{+}$ sufficiently decreased allowing $F_{Cu}$ to rupture the bridge. Curve labeled 0 shows uninterrupted sweep back to 0 V.

The switching behavior shown in Fig. 1(b) was performed under a low compliance current of 10 $\mu$A. An analogous switching behavior of the cell under a high compliance current is shown in Fig. 3(a) and reveals an interesting phenomenon. The voltage is repeatedly swept first from 0 V to 1 V. Abrupt switching from high resistance state to a low resistance state at SET voltages between 0.28 V and 0.34 V is observed exhibiting a sharp increase in current. Beyond $V_{set}$ the relation between current and voltage is linear. The slope corresponds to a resistance of $R_{on,2} = 7\,k\Omega$. When the voltage is swept from 1 V back to 0 V, the curve with almost the same slope of 7 k$\Omega$ is retraced below $V_{set}$ up to a voltage range of $0.11\,V < V_{trans} < 0.15\,V$. Within this narrow voltage range, a gradual transition is observed to a linear Ohm's behavior with a ten times higher slope corresponding to $R_{on,1} = 700\ \Omega$. The $R_{on,1}$ is of the same magnitude as the ON state resistance observed in Fig. 1(b) and $R_{on,2}/R_{on,1} \approx 10$. The transition between these two regions takes place in a rather narrow voltage range of about 0.04 V.

The explanation of the two slopes is consistent with the $F_{Cu} - F_{Cu}{}^{+}$ flux model discussed above in reference to Fig. 2(a). With the positive voltage sweep beginning at 0 V, at $V_{set}$ the Cu CF is being formed. It can be assumed that the bridge thus formed has a low resistance of the order of 1000 $\Omega$. As soon as the bridge is established, substantial current in excess of 200 $\mu$A is surging through the bridge leading to Joules heating and local hot spot temperatures. The elevated temperature enhances Cu diffusion at the base of the Cu bridge with the $\delta$-Cu layer leading to a weakening of the bridge and hence to its resistance increase. Since, at a given voltage, the power is given by $P = V^2/R$, the bridge seeks to stabilize itself by limiting the Cu atom loss to the Cu $\delta$-layer. With increased resistance the power and temperature both decrease and the fluxes of Cu ions and Cu atoms and can be balanced again. During the voltage sweep back the bridge is more or less stable, characterized by the $R_{on,2}$ resistance. However, below approximately 0.14 V, the reduced Joule heating decreases the $F_{Cu}$ flux. The $F_{Cu}$ flux is now smaller than the Cu ion flux $F_{Cu}{}^{+}$ and the bridge can be rebuilt to the full strength seen in Fig. 4 of about 700 $\Omega$. Importantly, the device under these circumstances exhibits still volatile behavior. When the voltage is swept to 0 V or to sufficiently small volatge values below 0.1 V, the bridge dissolves spontaneously. At sufficiently small voltages, the $F_{Cu}{}^{+}$ flux is too small to replenish the Cu atoms in the bridge that are lost due to diffusion at the CF/Cu $\delta$-layer interface.

When the same device is operated at high current of about 1 mA, a transition from volatile to nonvolatile switching is observed. In Fig. 3(b), the same device as in Fig. 3(a) has been tested under a high compliance current of 1 mA. The Cu bridge becomes now nonvolatile and a RESET operation is needed to rupture the bridge. The $V_{reset}$ voltage is about $-0.6$ V. After the RESET, the device can be again

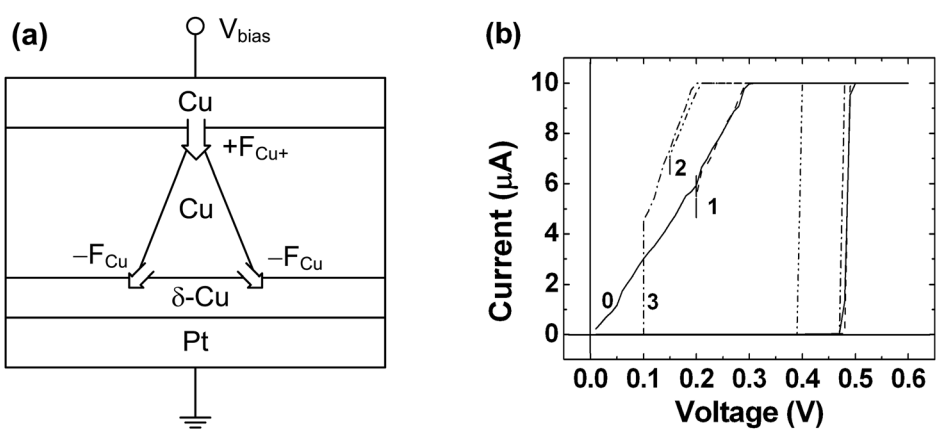


FIG. 2. (a) Conceptual view of the $Cu^{+}$ and Cu fluxes in volatile switching devices. (b) Resistive state transition during the volatile switching operations. For curves 1, 2, and 3, the sweep is halted at a small but non-zero voltage.

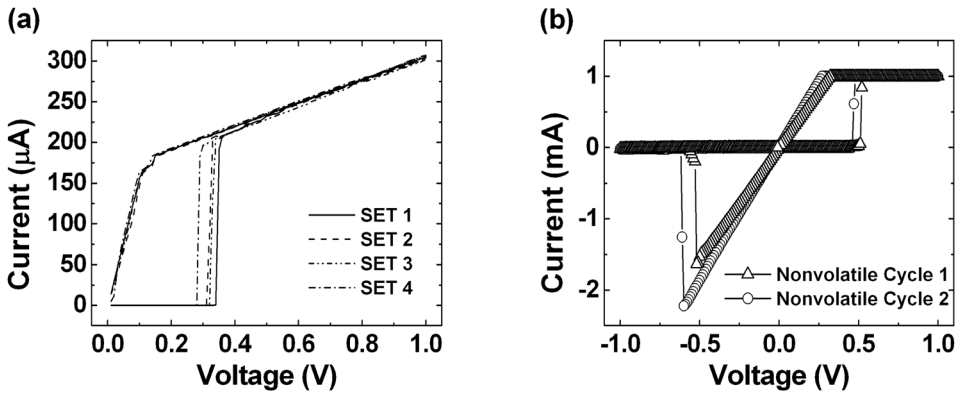


FIG. 3. (a) Volatile resistive switching without compliance current. (b) Nonvolatile switching of Cu/$TaO_x$/$\delta$-Cu/Pt device at high compliance current.

reliably operated in the volatile mode if the compliance current is below several hundreds of $\mu$A and characteristics as shown in Fig. 1(b) are fully recovered. Thus the $\delta$-Cu device can be switched reliably from volatile to nonvolatile I−V behavior. The semiconductor diode-like behavior of the volatile resistive switch allows now for implementation of AND and OR logic gates, similar to the well-known diode-transistor logic gates[8] with volatile and non-volatile resistive switches within the same crossbar array and without the need of providing a silicon substrate to accommodate semiconductor diodes. With one additional mask for the deposition of the $\delta$-Cu layer one can render predetermined cells within the crossbar array to become volatile while the remaining resistive switches to display non-volatile behavior. A volatile switch in a serial connection of volatile and non-volatile switches can also now supplant the Si diode selector with ReRAM.[9]

In Fig. 4(a), the switching time $\tau$ is shown for a constant applied voltage at various values between 0.35 V and 0.5 V. The voltage changes with a step of 0.025 V. It can be seen that as the voltage increases, the transition from HRS to LRS becomes less abrupt. The switching time $\tau$ can be fitted by an exponential function $\tau = \tau_0 \exp(-V/V_0)$ as shown in Fig. 4(b). The exponential relation has been explained by the migration of $Cu^+$ ions, the redox reaction on the electrode, and the nucleation of Cu atoms.[10–12]

In the following, the volatile switching behavior has been characterized and compared with nonvolatile switching. The SET voltages at different voltage ramp rates are shown in Fig. 5(a). In contrast to conventional nonvolatile devices,[13] $V_{set}$ is largely independent of the voltage ramp rate. Compared to conventional Cu/$TaO_x$/Pt devices, $V_{set}$ is significantly lower for Cu/$TaO_x$/$\delta$-Cu/Pt devices, which makes them interesting for low power applications. Similarly to the nonvolatile resistive switches, the ON-state resistance $R_{on}$ depends on the compliance current $I_{cc}$ during the SET operation. The relation can also be fitted by a reciprocal function, $R_{on} = K/I_{cc}$, as shown in Fig. 5(b). The distributions of $R_{on}$, $R_{off}$, and $V_{set}$ are shown in Figs. 5(c) and 5(d). As it can be seen from Fig. 5(c) and 5(d), with the Cu $\delta$-layer, we obtain tighter distribution of $V_{set}$, $R_{off}$, and $R_{on}$ than for nonvolatile Cu/$TaO_x$/Pt devices. The improvement in $V_{set}$ distribution of the volatile $\delta$-Cu device over the conventional nonvolatile devices is tenfold (see Fig. 5(d)). In general, the insertion of a Cu $\delta$-layer with adjusted thickness below 6.5 nm offers a control parameter to optimize also nonvolatile switching behavior with much tighter $V_{set}$, $R_{off}$, and $R_{on}$ distributions than the conventional devices.

The transition from nonvolatile to volatile behavior is governed by the balance between transport of Cu atoms and ions. The magnitude of Cu atom flux is impacted by the existence and thickness of the Cu $\delta$-layer. For compliance current below 100 $\mu$A, a single ON-state resistance $R_{on}$ characterizes the I−V curves. For high compliance current, the I−V characteristics are characterized by two ON resistance states $R_{on,1}$ and $R_{on,2}$. $R_{on,1}$ corresponds to the $R_{on}$ for volatile resistive switching under low compliance currents. The $R_{on,2}$ resistance characterizes the I−V behavior after the bridge is formed at $V_{set}$ and is operated at voltages beyond $V_{set}$. During the negative voltage sweep back to zero, the $R_{on,2}$ curve is retraced up to a voltage $V_{trans} < V_{set}$, where the curve changes the slope in a narrow voltage interval to a slope characterized by $R_{on,1}$. Transition from volatile to nonvolatile switching can be effectuated by imposition of a high enough compliance current. The volatile cells are characterized by a retention time smaller than 0.5 s as dictated by the voltage sweep rate, whereas the

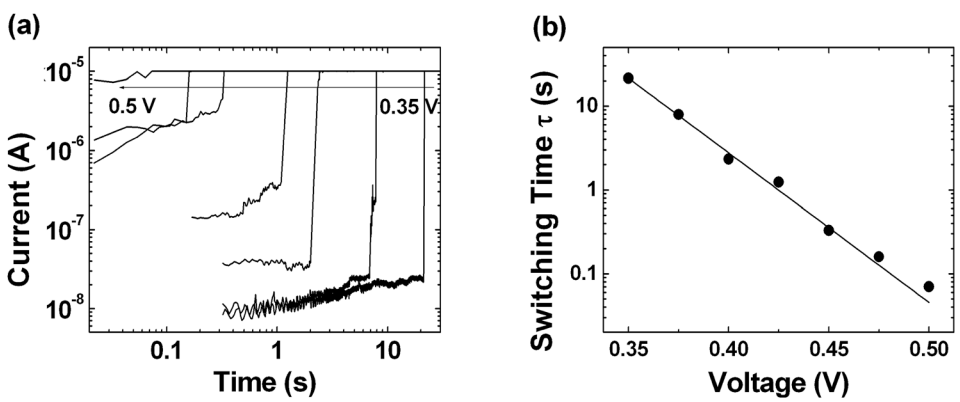


FIG. 4. (a) I-t characteristics of the volatile device. The device is biased at constant voltages with the step of 0.025 V. (b) Dependence of switching time on bias voltages of the volatile Cu bridge.

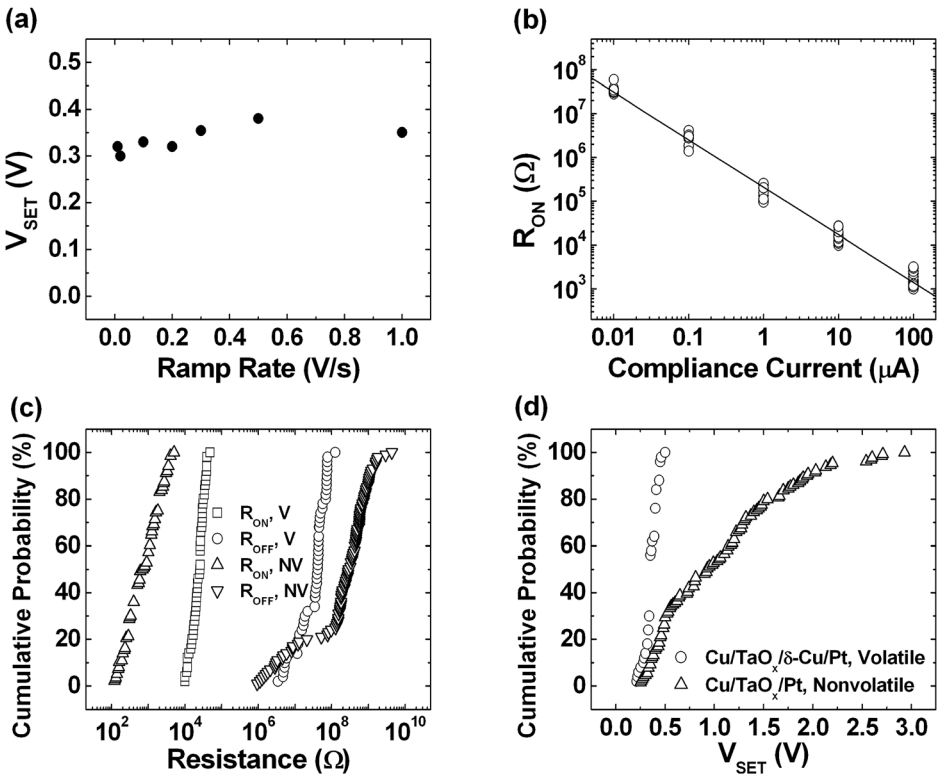


FIG. 5. (a) $V_{set}$ of volatile switching devices at different ramp rates. (b) Dependence of $R_{on}$ on compliance current of the volatile Cu bridge. (c) $R_{on}$ and $R_{off}$ distributions of volatile (V) and nonvolatile (NV) devices. (d) $V_{set}$ distribution of volatile and nonvolatile devices.

retention for nonvolatile devices is at least $10^6$ s. The volatile resistive switching device enables very compact realization of volatile and nonvolatile RRAM in the same device including switching between the two modes of operation and opens areas of applications in logic circuits, memristive and chaotic circuits, and neural networks. Since the I–V characteristic of a volatile resistive switch resembles I–V characteristic of a diode, a cross point array of nonvolatile and volatile switches enables not only the functionality of nonvolatile memory but also of the diode-based logic analogous to diode-transistor logic.[8] Thus, both memory and logic functions can be realized by the same type of resistive device removing the constraint of manufacturing these devices on silicon substrates.

[1]R. Waser and M. Aono, Nature Mater. **6**(11), 833 (2007).
[2]S. Kaeriyama, T. Sakamoto, H. Sunamura, M. Mizuno, H. Kawaura, T. Hasegawa, K. Terabe, T. Nakayama, and M. Aono, IEEE J. Solid-State Circuits **40**(1), 168 (2005).
[3]J. Borghetti, G. S. Snider, P. J. Kuekes, J. J. Yang, D. R. Stewart, and R. S. Williams, Nature **464**, 873 (2010).
[4]S.-J. Choi, G.-B. Kim, K. Lee, K.-H. Kim, W.-Y. Yang, S. Cho, H.-J. Bae, D.-S. Seo, S.-I. Kim, and K.-J. Lee, Appl. Phys. A **102**(4), 1019 (2011).
[5]M. Itoh and L. Chua, Int. J. Bifurcation Chaos **18**(11), 3183 (2008).
[6]T. Liu, M. Verma, Y. Kang, and M. K. Orlowski, IEEE Electron. Device Lett. **33**(3), 429 (2012).
[7]Q. Liu, C. Dou, Y. Wang, S. Long, W. Wang, M. Liu, M. Zhnag, and J. Chen, Appl. Phys. Lett. **95**, 023501 (2009).
[8]D. Neamen, *Microelectronics Circuit Analysis and Design* (McGraw Hill, 2009).
[9]X. Tran, H. Yu, Y. Yeo, W.Liu, Z. Wang, Z. Fang, K. Pey, X. Sun, A. Du, B. Nguyen, and M. Li, IEEE Electron. Device Lett. **32**(3), 396 (2011).
[10]K. Terabe, T. Hasegawa, T. Nakayama, M. Aono, Nature **433**, 47 (2005).
[11]U. Russo, D. Kamalanathan, D. Ielmini, A. L. Lacaita, and M. N. Kozicki, IEEE Trans. Electron. Devices **56**(5), 1040 (2009).
[12]J. R. Jameson, N. Gilbert, F. Koushan, J. Saenz, J. Wang, S. Hollmer, and M. N. Kozicki, Appl. Phys. Lett. **99**, 063506 (2011).
[13]C. Schindler, G. Staikov, and R. Waser, Appl. Phys. Lett. **94**, 072109 (2009).